Supplementary Information
The simplicity of planar networks

MP Viana, E. Strano, P. Bordin, M. Barthelemy

I. DATASETS

A. Static networks

Oxford and Bologna The street networks of these two cities have been downloaded from Open Street Map [1]. They represent all streets including local urban streets and major roads. The boundaries of the networks were determined by the gradient of built-area density and include a minor peripheral zone of non urban streets.

Nantes The Nantes water system was extracted from a more global dataset: 'eau-tuyau', managed by Nantes Metropole. This dataset is copyrighted by Nantes Metropole and have been granted to us for research purposes only.

The Nantes road network was extracted from the map 'BD Topo 2013' from the french national mapping agency. It is copyrighted by the IGN (Institut Geographique National).

Australian highways network This network represents the full highway system of Australia and is part of the global road network from *Data and Maps for Server* provided by ESRI ArchGis under official ArchGis license. The data are ESRI copyrighted and have been granted for research purpose as described in the ESRI Proprietary Rights Acknowledgment [2].

UK rail network This network represents the full rail transportation system in the UK. This dataset is in the public domain under the ODC Public Domain Dedication and Licence (PDDL) [3] and has been downloaded from the website ShareGeoOpen [4].

Leaves *Ilex Aquifolium* has been visually extracted using scanned imaged of cleaned leaf of Ilex aquilfolium visible in the collection of natural picture callPhoto [5].

Wing The vascular system of an anterior wing of a dragonfly was digitilized with a high resolution scanner. The insect was collected in the region of Aquasanta, Liguria (Italy), in June 2005. This dragonfly seems to belong to the family of Gomphidae.

Evolving networks

Groane The area under study, known as Groane, covers a surface of $125km^2$, includes 29 urban centres within 14 municipalities, and has essentially evolved along two main radial paths, connecting Milan to Como and Milan to Varese. In the last two centuries, the Groane area has faced a complex process of conurbation, changing from a polycentric region into a completely urbanised area which is a common process for many large European metropolitan regions. Despite local differences, it is possible to identify four distinct phases that characterize urbanization in this area:

- (i) Rural phase, (1800–1918): fundamentally pre-industrial, fully based on agricultural economy, with no major transportation infrastructures present.
- (ii) Early-urban phase (1918–1945): between world wars period, still significantly based on agriculture economy, witnessing the first appearance of rail network, first small-scale sparse industrial colonisation, and limited expansion of rural settlements around the historical centres.
- (iii) Urban-industrial phase (1945–1990): remarkable sprawled residential and industrial development (especially textile and mechanics) along with population growth and highway construction.
- (iv) Metropolitan post-industrial phase (1990–2012): decline of industrial activities, slower-paced urban sprawl, former polycentric organisation overwhelmed by the metropolitan continuum caused by the merging of expanded centres, increased long-range mobility due to the development of high speed trains and large highway systems.

By importing historical topographical and photogrammetrical data into a Geographical Information System (GIS) environment, we reconstructed the detailed road system (including minor streets) at seven different points time points: 1833, 1914, 1933, 1955, 1980, 1994, 2007 (see [6] for more details).

Paris dataset By digitizing historical maps into a GIS environment, we reconstructed the detailed road system (including minor streets) at five different time points: 1789, 1826, 1836, 1888, 1999. In particular, it is important to note that we have thus snapshots of the

street network before Haussmann works (1789-1836) and after (1888-2010). This allows us to study quantitatively the effect of such central planning. See also [7] for more details.

The networks for 1789, 1826, 1836, 1888 are extracted from the following maps:

- 1789: Map of the city of Paris with its new enclosure. Geometrically based on the 'meridienne de l'Observatoire' and surveyed by Edmé Verniquet. Finished in 1791.
- 1826: Road map of Paris surveyed by Charles Picquet, geographer for the King and the duke of Orléans.
- 1836: Cadastre of Paris, Philibert Vasserot. Map constructed according to blocks and classified according to old districts. 24 Atlas, 1810-1836.
- 1888: Atlas of the 20 districts of Paris, surveyed by M. Alphand, and L. Fauve, under the administration of the prefect E. Poubelle, Paris, 1888.

All these maps were digitized at the LaDéHiS under the supervision of Maurizio Gribaudi, in the framework of a research on the social and architectural transformations of parisian neighborhoods between the 18th and 19th centuries. The network extracted from the Vasserot cadastre was initiated by Anne-Laure Bethe for the program Alpage [8].

The networks of 1999 is from the french Geographical National Institute (IGN) on the basis of modern surveys.

Physarum Policephalum This Physarum Policephalum plasmodium has been cultivated under sterile environment in a 10 cm radius Petri dish [9]. The Petri dish was kept in a dark at approximately 22 degrees for a period of 48 hours. Active plasmodium has been inoculated over a single food source composed by sterilized oat flour tablets of 3mm radius. High resolution pictures were taken every then minutes. Five snapshots were chosen for analysis and their respective network were drawn on ArchMap software based on visual inspection. Only tubes thicker than 0.3 mm were considered.

A summary of all networks used in this article and some of their relevant attributes as well are reported in Table 1.

Network	N	N^*	$\langle l \rangle$	$\langle l^* \rangle$	D	D^*	$\langle k \rangle$	$\langle k^* \rangle$	d_{max}	S
UK railway system	1848	1103	31.0	10.0	91	36	2.7	3.7	951km	1.149
Australia highway system	1767	1166	27.3	11.1	64	24	3.1	4.3	4469km	1.273
Bologna	5200	2637	40.1	6.63	112	18	2.6	3.5	15.6km	1.148
Oxford	4372	2491	33.1	7.65	74	21	2.3	2.9	14.2km	1.192
Nantes	675	420	17.0	5.73	38	13	2.9	4.0	4.7km	1.271
Nantes water system	1255	721	27.7	8.41	72	20	2.1	2.5	4.0km	1.286
Leaf (*Ilex aquifolium*)	1131	833	18.3	6.28	43	13	2.5	3.4	3.5cm	1.430
Leaf (*Hymenanthera chathamica*)	11870	8730	40.0	10.5	91	23	2.3	3.1	3.4cm	1.420
Dragonfly	1271	1093	25.6	5.60	63	13	3.0	4.1	2.6cm	1.758
Groane 1833	255	140	10.7	4.46	25	10	2.7	3.7	15.4km	1.118
Groane 1914	805	419	19.4	5.39	46	12	2.6	3.4	16.1km	1.121
Groane 1933	948	499	21.3	5.05	49	11	2.6	3.5	16.1km	1.140
Groane 1955	2268	1160	31.0	5.71	72	13	2.7	3.8	16.1km	1.157
Groane 1980	4104	2096	34.5	6.00	81	14	2.8	3.9	16.1km	1.298
Groane 1994	4419	2291	34.6	5.99	78	13	2.8	4.0	16.1km	1.284
Groane 2007	5004	2607	36.7	6.03	84	15	2.8	4.0	16.1km	1.299
Paris 1789	1935	977	24.4	5.30	67	13	3.0	4.3	8.9km	1.320
Paris 1826	2466	1237	25.5	5.72	58	13	3.0	4.5	8.9km	1.267
Paris 1836	2784	1399	26.7	5.54	57	13	3.0	4.3	8.9km	1.290
Paris 1888	5100	2342	34.3	4.72	84	12	3.2	5.2	8.9km	1.273
Paris 1999	5215	2391	34.0	4.76	80	12	3.2	5.3	8.9km	1.258
Physarum h04	162	106	9.17	5.56	20	12	2.3	3.1	0.61cm	1.040
Physarum h08	247	180	11.4	6.46	27	14	2.6	3.4	0.70cm	1.076
Physarum h10	427	303	14.3	6.70	32	15	2.7	3.6	0.75cm	1.116
Physarum h15	317	233	11.8	6.58	25	14	2.5	3.4	0.83cm	1.097
Physarum h20	441	297	14.7	6.45	31	15	2.5	3.4	1.35cm	1.085

TABLE I: Networks used in this report. Number of nodes N, average topological shortest path length $\langle l \rangle$, network diameter D, average node degree $\langle k \rangle$, maximum euclidean distance between two pair of nodes d_{max}, and simplicity index S. Symbol $*$ is used for measurements calculated over the dual representation.

II. STATISTICS FOR THE NUMBER OF TURNS

We display here the probability distribution $P(\tau)$ that a given path has τ turns. The distribution has been calculated for all shortest and simplest paths for the networks of Paris (1999) and of the leaf *Ilex aquifolium* and the results are shown in Fig. 1(a). These results

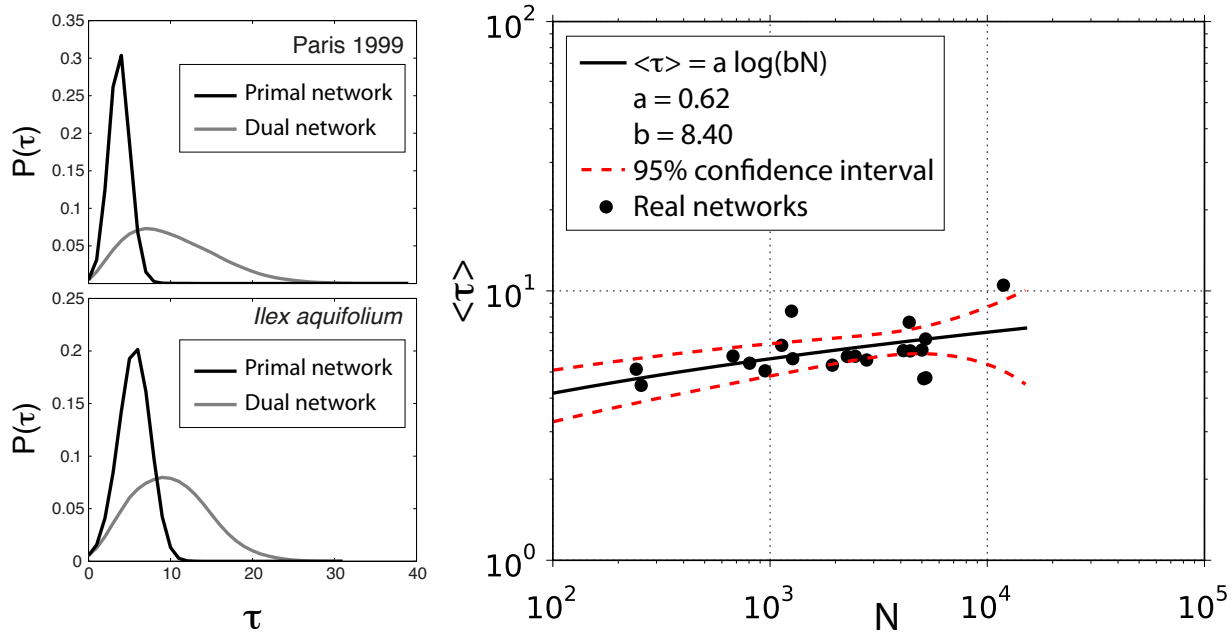

FIG. 1: (a) Probability distribution of number of turns for Paris (1999), a leaf (Ilex aquifolium). (b) Average number of turns $\langle\tau\rangle$ versus the size of the network N for all the networks studied here. The fit here is logarithmic showing a very slow dependence of τ versus N, a behavior typical of small-world networks.

confirm that the number of turns along simplest paths is smaller than for shortest paths, as expected. In addition, it can be seen that $P(\tau)$ for the simplest paths is well fitted by a normal distribution centered in $\tau_c \approx 6$ turns, which means that on average, any pair of nodes is separated by a simplest path made of 6 turns, regardless the nature of the network (Paris or Ilex).

We also show in Fig. 1(right panel) the average number of turns $\langle\tau\rangle$ as a function of the number of nodes N which displays a small-world type behavior characterized by a slow logarithmic increase with N.

III. A NULL MODEL

In order to have a simple benchmark to compare our networks with, we introduce the following model. The model starts with N points randomly distributed in a square of unit area. We then construct the Voronoi graph on these points (Voronoi edges that fall out of the square are ignored). Next, we add a tunable fraction of straight lines of length distributed according to $P(\ell) \sim \ell^{-\alpha}$. We show in Fig. 2 of this SI the results for $\alpha = 0$. The density of straight lines ρ is defined as the ratio $\rho = L_{SL}/L$ where L_{SL} is the total length of straight lines. The total network length L is given by $L = L_{SL} + L_{se}$, where L_{se} corresponds to the total length of single edges (not belonging to any straight line) shown in gray in Fig. 2. If a given node in the dual representation represents a unique edge in the primal representation we call this edge, a single edge.

The calculation of the simplicity could be computationally costly and we checked that a small samples of pairs of nodes is enough to compute accurately the simplicity index. In Fig. 3 we represent the convergence versus the fraction of pairs of nodes used to compute the index. We see that for a small fraction such as 2.5% we already have an accuracy of 10^{-3}. It is important to observe that this approximation was only used for the model and that the simplicity index for real networks is exact.

We show in Fig. 4, the simplicity profile obtained for the model for $\alpha = 0$ and $\alpha = 2$ for different values of the density of straight lines. In both cases, we see a non monotonous behavior when the density is increased: for low density, we have a small simplicity and for a large density there are enough straight lines to provide a simple path not too different from the shortest one. The value of the peak d^* decreases with the density, consistently with the picture that d^* represents the size of domains 'free' of long straight lines.

We finally note that the effect of straight lines is more pronounced in the case $\alpha = 0$ where their length displays a wider variety than in the case $\alpha = 2$.

---

[1] http://downloads.cloudmade.com/.

[2] http://www.esri.com/LEGAL/COPYRIGHT-TRADEMARKS

[3] http://opendatacommons.org/licenses/pddl/1.0/

[4] http://www.sharegeo.ac.uk/handle/10672/49?show=fullindate30-08-2013.

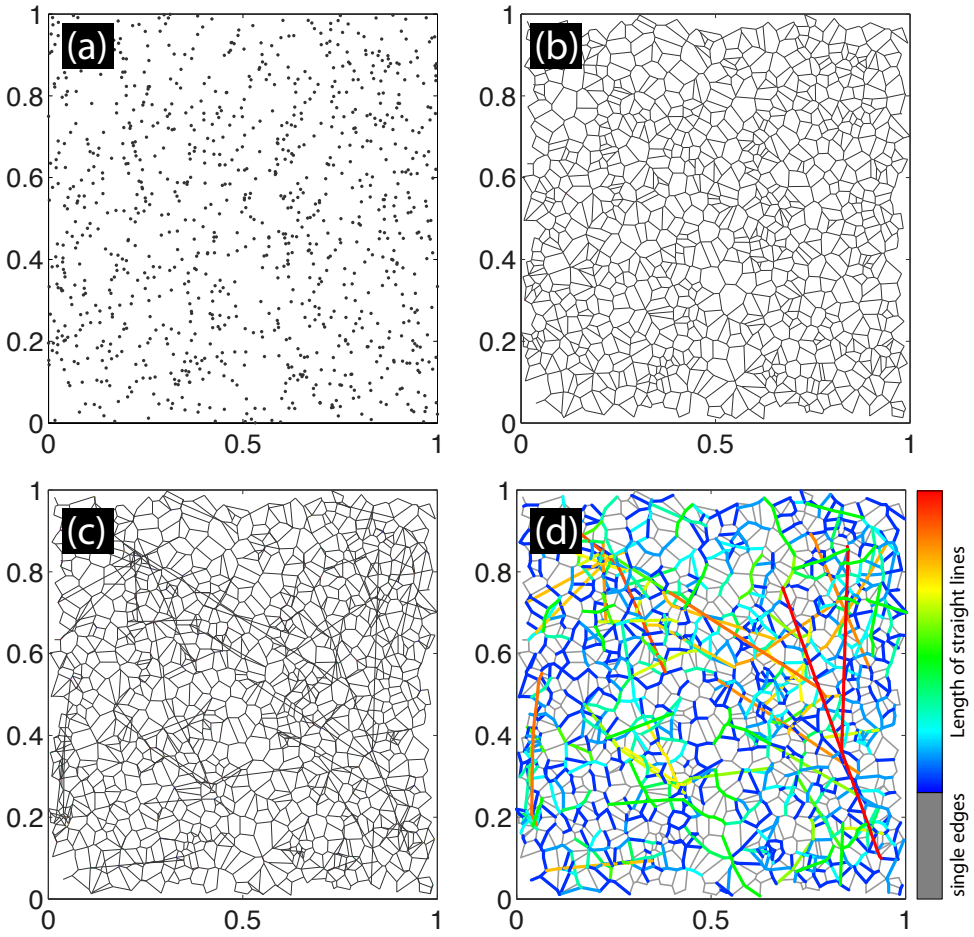

FIG. 2: Illustration of the model: We start from a random set of points (a), construct the Voronoi lattice over this set (b) and add straight lines of random lengths and random locations. In (d) we indicate the straight lines with a color code according to their length, and single edges are represented in gray.

[5] `http://calphotos.berkeley.edu/`

[6] Strano E, Nicosia V, Latora V, Porta S, Barthelemy M (2012) Elementary processes governing the evolution of road networks. *Scientific Reports* 2:296.

[7] Barthelemy M, Bordin P, Berestycki H, Gribaudi M (2013) Self-organization Self-organization versus top-down planning in the evolution of a city. *Scientific Reports* 3:2153.

[8] A.L. Bethe, Vasserot voies (1810-1836), ALPAGE, 2009.

[9] Nakagaki T, Kobayashi R, Nishiura Y, Ueda, T (2004) Obtaining multiple separate food sources: behavioural intelligence in the Physarum plasmodium. *Proceedings of the Royal Society of London. Series B: Biological Sciences* 271:2305-2310.

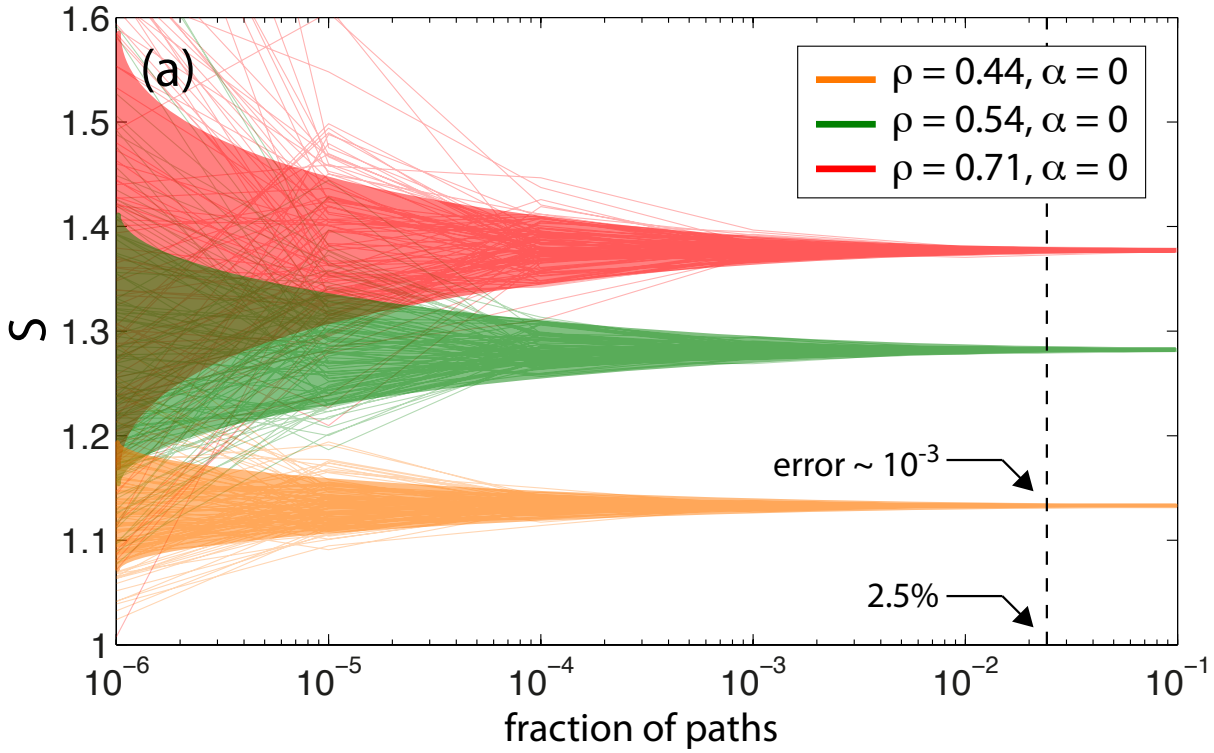

FIG. 3: (a) Illustration of the convergence of the simplicity calculation versus the fraction of pairs of nodes used.

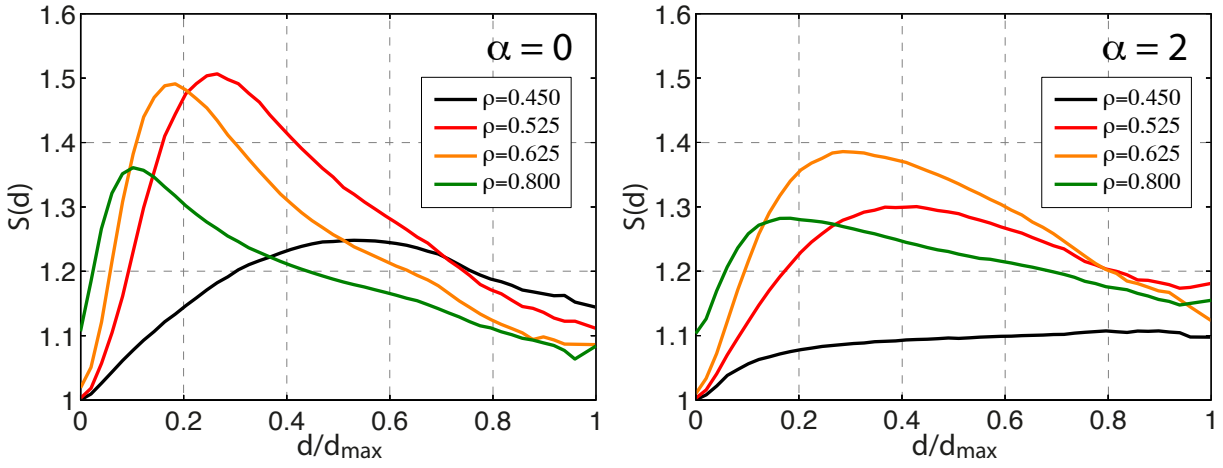

FIG. 4: Profiles for the null model for different values of α: (a) $\alpha = 0$ and (b) $\alpha = 2$ and for different values of the density of straight lines.